Adsorption and Photochemistry of CF2Br2 (Halon 1202) on Highly Ordered Pyrolytic Graphite (HOPG)

ARTICLE *in* THE JOURNAL OF PHYSICAL CHEMISTRY B · NOVEMBER 2000

Impact Factor: 3.3 · DOI: 10.1021/jp002374k

3 AUTHORS, INCLUDING:

Michael Dorko
The Citadel
8 PUBLICATIONS **65** CITATIONS
SEE PROFILE

Simon J. Garrett
California State University, Northridge
30 PUBLICATIONS **417** CITATIONS
SEE PROFILE

Adsorption and Photochemistry of CF_2Br_2 (Halon 1202) on Highly Ordered Pyrolytic Graphite (HOPG)

Michael J. Dorko, Todd R. Bryden, and Simon J. Garrett*

Department of Chemistry, Michigan State University, East Lansing, Michigan 48824

Received: July 3, 2000; In Final Form: October 16, 2000

The adsorption and photochemistry of dibromodifluoromethane (Halon 1202) adsorbed on highly ordered pyrolytic graphite (HOPG) was studied using temperature-programmed desorption (TPD), X-ray photoelectron spectroscopy (XPS) and electron energy loss spectroscopy (EELS). Dibromodifluoromethane adsorbs molecularly at 85 K and the first layer saturates at a fractional coverage of 0.14 ± 0.01 monolayer (ML). Molecular desorption occurs at ~140 K (monolayer) and ~110 K (multilayers) with desorption energies of 43.8 ± 4.6 and 22.4 ± 1.9 kJ/mol, respectively. Ultraviolet irradiation of the monolayer by a filtered Hg-arc lamp (225−350 nm) resulted in the formation of CF_2Br and Br (major products) and Br_2 and $C_2F_4Br_2$ (minor products). The estimated integrated dissociation cross-section was 1.9×10^{-19} cm^2, close to the calculated value for CF_2Br_2(g) (4.5×10^{-19} cm^2). The similarity of these two values implies that photodissociation of CF_2Br_2(ad)/HOPG is dominated by direct photoabsorption of the adsorbate and not electronic processes moderated by the substrate. The influence of the surface is most clearly observed in the distribution of products measured by TPD. We attribute the differences observed between adsorbate and gas phase/matrix isolation experiments to the high density of photogenerated species trapped in the surface layer.

I. Introduction

During the past two decades, it has become increasingly apparent that heterogeneous reactions on particulate surfaces play an important role in atmospheric chemistry. For example, it has been shown that catalytic reactions on polar stratospheric cloud and nitric acid trihydrate surfaces contribute to the destruction of stratospheric ozone.[1−4] These surfaces provide a medium upon which photoactive reservoir molecules (the oxidation products of atmospheric halocarbons) are produced more readily than in the gas phase alone. Photolysis of these species in the stratosphere provides halogen atoms that can catalyze ozone destruction.

A variety of natural and anthropogenic sources of halogenated molecules in the atmosphere include chlorofluorocarbons (refrigerants, foam-blowing agents, solvents) and fully halogenated bromomethanes and bromoethanes (Halons, fire retardants). The presence of brominated molecules in the atmosphere is particularly noteworthy since the ozone depletion potential (ODP) of these molecules is larger than their chlorinated analogues.[5] The most common brominated molecules are CH_3Br (up to about 10 ppt) and various Halons (total up to about 7 ppt).[6] Since removal of Halons occurs exclusively by short wavelength photolysis, many have relatively long atmospheric lifetimes (5−100 years)[7] and so are efficient means of halogen mass transport to the stratosphere. Because of their role in stratospheric ozone loss, most of these molecules have been restricted by international agreement.[8] Currently, Halon 1202 (CF_2Br_2) is not regulated by this agreement. Indeed, the atmospheric concentration of Halon 1202 has recently begun to rise by significant amounts, prompting debate over its environmental origin.[9]

The primary goal of the present study was to determine whether the photochemistry of CF_2Br_2 is altered when it is adsorbed on a model carbonaceous aerosol surface (highly ordered pyrolytic graphite, HOPG). While the photochemistry of halogenated compounds on ice, sulfuric acid and sea-salt surfaces have been the subject of many investigations,[1−4,10−14] reactions occurring on carbonaceous aerosols have been largely unexplored. These aerosols form the most abundant particulates over continents with the global load estimated at about 270×10^6 kg.[15] Their chemical composition is highly variable, depending upon their formation process and history in the atmosphere. The so-called primary organic aerosols (soot, graphitic carbon and carbon black) are structurally similar to impure graphite and are usually formed as a result of combustion processes.

If enhanced photodissociation cross sections for brominated adsorbates occur, the importance of aerosol chemistry as a net source for bromine atoms in the atmosphere will increase. In contrast, the ODP for Halons may be decreased if chemisorption of halogen atoms on the carbon particulate surface creates a net sink. In our experiments we use HOPG as a model for the surface of primary carbon particulates. Depending upon energetic coupling between the adsorbate and substrate, the semimetallic electronic structure of the graphite may significantly perturb the photochemistry of an adsorbed molecule.[16]

II. Experimental Section

A detailed description of the experimental apparatus has been given elsewhere.[17] All experiments were performed in two connected stainless steel ultrahigh vacuum (UHV) chambers with an overall base pressure of 2×10^{-10} Torr. X-ray photoelectron spectroscopy (XPS) and temperature-programmed desorption (TPD) measurements were made in the first chamber. This chamber contained a molecular leak valve, quadrupole mass spectrometer (QMS), a dual anode (Mg/Al K$\alpha_{1,2}$) X-ray source, and a hemispherical electron energy analyzer. The second chamber, which was double μ-metal shielded, contained a high-resolution electron energy loss spectrometer (EELS).

10.1021/jp002374k CCC: $19.00
Published on Web 11/17/2000

An HOPG sample (grade SPI-2, SPI Supplies) measuring 10 × 10 × 1 mm was mounted on a long-travel manipulator capable of x, y, z, translation and θ rotation. The sample was secured to a molybdenum mount by two titanium clips, under one of which was placed an E-type thermocouple directly in contact with the sample face. The sample could be heated to >800 K by a tungsten filament embedded in the molybdenum mount and cooled to <85 K using liquid nitrogen.

The HOPG was repeatedly cleaved using adhesive tape to expose a fresh, visibly flat C(0001) surface and then outgassed at 720 K in UHV for 5−6 h. Such a procedure is known to produce clean, ordered C(0001) surfaces.[18] Prior to each day's experiments, the sample was flashed to ~800 K to remove any accumulated adsorbates. X-ray photoelectron spectroscopy measurements showed up to 3% oxygen-containing species were present on the surface after flashing.

The clean HOPG surface was cooled to 85 ± 1 K and exposed to CF_2Br_2 (~98%, PCR Research Chemicals, Inc.) by backfilling the UHV apparatus. The CF_2Br_2 was used without further purification. All CF_2Br_2 exposures are given in Langmuirs (1 langmuir ≡ 10^{-6} Torr·s) and are uncorrected for ion gauge gas sensitivity.

All TPD spectra were recorded over a temperature range of 85−450 K with a linear heating rate of 10 K/s. Molecules were transmitted to the QMS through a 2 mm diameter aperture in a stainless steel shroud enclosing the ionizer. Desorbing molecules were collected along the surface normal which was coincident with the QMS line-of-sight.

The adsorbate-covered surface was exposed to unpolarized UV irradiation from a medium-pressure Hg-arc lamp (Oriel 6286) operated at 350 W. The lamp was equipped with a condenser lens and a visible/infrared liquid filter (~1 M $NiSO_4$ solution) that primarily transmitted wavelengths in the range between 225 and 350 nm. The UV radiation was introduced into the UHV apparatus through a fused quartz window such that its angle of incidence was 45° with respect to the surface normal. An aperture (12.7 mm diameter) affixed to the window minimized irradiation of the sample mount. A power of 8.6 mW/cm^2 was measured at the sample-lamp distance by a thermopile detector. All UV irradiation of the adsorbate-covered surface were performed at a surface temperature of ≤85 K. Upon exposure to the UV radiation, the surface temperature increased by ~6 K. No evidence was observed for thermally driven reactions under these modest temperature increases.

All XP spectra were collected using the Mg K$\alpha_{1,2}$ X-ray line ($h\nu$ = 1253.6 eV) operated at 300 W (15 kV, 20 mA) and an analyzer pass energy of 100 eV. To maximize surface sensitivity, photoelectrons were collected at a take-off angle of 65° from the surface normal. Spectra were referenced to the C 1s peak from HOPG at 284.7 eV binding energy (BE).[19] No changes in the photoemission data were observed during extended periods (up to 1 h) of X-ray irradiation. Typically, photoemission data (C 1s, F 1s, and Br 3d) were acquired in less than 20 min. After each spectral acquisition, the surface was flashed to 450 K and a fresh layer of CF_2Br_2 was dosed. A temperature of 450 K was found to be sufficient for removal of all F and Br from the surface after adsorption and UV exposure experiments as evidenced by XPS.

The CF_2Br_2 adsorbate was also characterized by high-resolution electron energy loss spectroscopy (EELS). Measurements employed a primary beam energy of 6.09 eV and a typical resolution (fwhm) of 51−54 cm^{-1}. All experiments were performed in the specular scattering geometry ($\theta_i = \theta_s = 55°$) with count rates from a clean HOPG surface of >10^6 Hz.

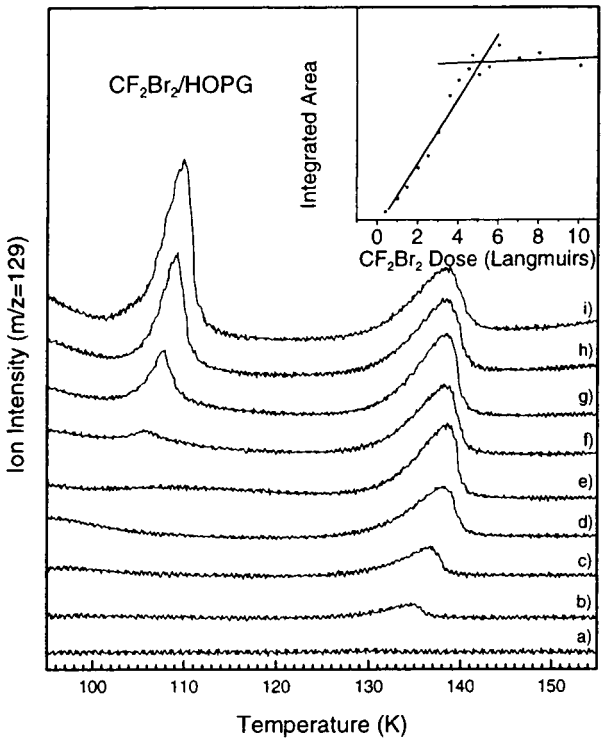

Figure 1. Temperature-programmed desorption data (m/z = 129, CF_2Br^+) for increasing exposures of CF_2Br_2 on HOPG. Exposures were (a) 0.4 langmuir, (b) 1.5 langmuir, (c) 2.5 langmuir, (d) 3.6 langmuir, (e) 4.5 langmuir, (f) 5.1 langmuir, (g) 6.1 langmuir, (h) 8.1 langmuir, and (i) 10.1 langmuir. Inset shows integrated area of the feature at ~140 K (monolayer) as a function of exposure.

III. Results

A. Temperature-Programmed Desorption. The adsorption behavior of CF_2Br_2 on HOPG was studied by TPD. Figure 1 shows a series of m/z = 129 (CF_2Br^+, base peak for CF_2Br_2) TPD spectra for increasing exposures of CF_2Br_2. Low exposures produced a broad desorption peak centered at 135 K, suggesting weak adsorbate−substrate interaction (physisorption). For progressively higher exposures this peak grew in area and the peak maximum shifted toward higher temperature, reaching 138 K after 4.8 langmuir of CF_2Br_2. This feature displayed a common leading edge with increasing exposure, indicative of zero-order desorption kinetics. A leading-edge analysis[20] of this feature indicated a desorption energy of 43.8 ± 4.6 kJ/mol.

As the CF_2Br_2 exposure increased, saturation of the peak at 138 K occurred indicating completion of the first adsorbed layer. The inset of Figure 1 shows a plot of integrated TPD area for this peak as a function of exposure. The area increased linearly and then remained approximately constant with additional CF_2Br_2. Linear fits to the increasing and constant regions yielded an intersection point of 4.8 langmuir and we use this exposure as equivalent to saturation of the first layer in subsequent discussions.

Exposures >4.8 langmuir lead to the appearance of a lower temperature desorption peak centered at 109 K. This peak did not saturate with increasing exposure and also exhibited a common leading edge. Such zero-order desorption kinetics are characteristic of multilayer desorption.[21] A leading-edge analysis of this peak, gave a desorption energy of 22.4 ± 1.9 kJ/mol.

Figure 2 shows TPD spectra for 4.8 langmuir CF_2Br_2 on HOPG measured at m/z = 31 (CF^+), 50 (CF_2^+), 79 (Br^+), 100 ($C_2F_4^+$), 129 (CF_2Br^+), 160 (Br_2^+), and 179 ($C_2F_4Br^+$). These ions were chosen because they are representative of the

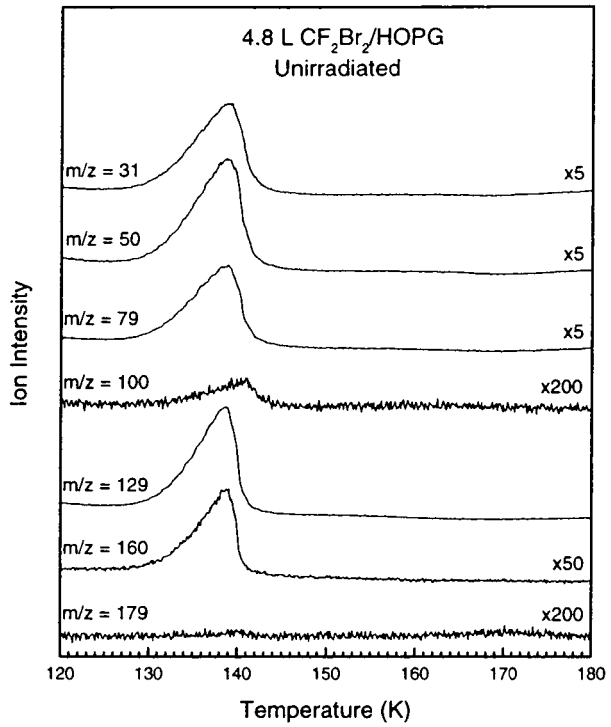

Figure 2. Temperature-programmed desorption data for 4.8 langmuir CF_2Br_2(ad)/HOPG. Monitored masses were $m/z = 31$ (CF^+), 50 (CF_2^+), 79 (Br^+), 100 ($C_2F_4^+$), 129 (CF_2Br^+), 160 (Br_2^+) and 179 ($C_2F_4Br^+$).

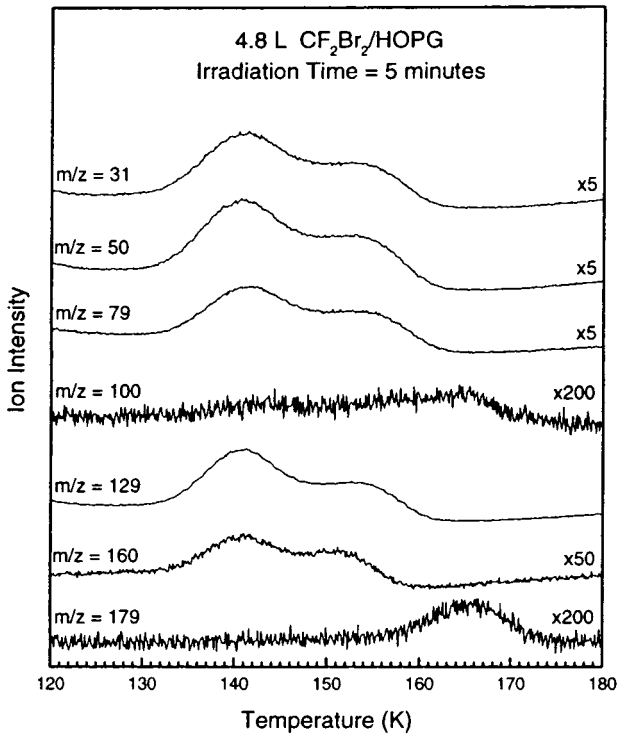

Figure 3. Temperature-programmed desorption data for 4.8 langmuir CF_2Br_2(ad)/HOPG, after 5 min of UV irradiation (filtered Hg-arc, 225−350 nm, incident power 8.6 mW/cm^2). Monitored masses same as Figure 2.

fragmentation pattern of gas-phase CF_2Br_2 and possible photolysis products. Each spectrum was obtained from a separate CF_2Br_2 exposure. Except for the $m/z = 100$ and 179 data, each ion had a similar desorption profile and peak temperature (138 K) suggesting a common origin. We concluded that molecular desorption occurred by comparison of the relative ion abundances for the TPD data presented here at $m/z = 31$, 50, 79, 129, and 160 (21:24:17:100:1.5) with the mass spectrum of gas-phase CF_2Br_2 (18:21:17:100:2) as measured by residual gas analysis. A small amount of $m/z = 100$ (<1% area of $m/z = 129$) was observed both in TPD measurements and residual gas analysis of the CF_2Br_2 admitted to the chamber indicating the presence of an unidentified contaminant. No signal was observed at $m/z = 179$.

A significant change in the TPD spectra was seen after UV irradiation of the adsorbate. Figure 3 shows a similar set of TPD spectra to those in Figure 2 after 5 min of UV irradiation. The monolayer peak originally present at 138 K broadened and shifted to 141 K and a second desorption peak centered at 155 K grew in for $m/z = 31$, 50, 79, 129, and 160. Relative ion abundances of 23:27:20:100:1.4 and 22:27:22:100:1.3 ($m/z = 31$, 50, 79, 129, and 160) for the 141 and 155 K peaks, respectively, indicated that each peak was associated with molecular CF_2Br_2. The $m/z = 100$ and 179 TPD spectra showed a broad desorption peak at ~165 K. These features are associated with the formation of a photolysis product, $C_2F_4Br_2$, as will be discussed later.

Figure 4 shows TPD spectra of the previously monitored ions after 15 min of UV irradiation. The peak originally present at 141 K for $m/z = 31$, 50, 79, and 129 in Figure 3 shifted to a higher desorption temperature (~146 K) and had started to merge with the leading edge of the peak at 155 K. The peak at 155 K was present for all UV exposures up to 60 min (data not shown). Furthermore, a comparison of the $m/z = 160$ TPD spectra in Figures 3 and 4 revealed the growth of a new peak at 165 K with continued UV exposure. This new peak in the

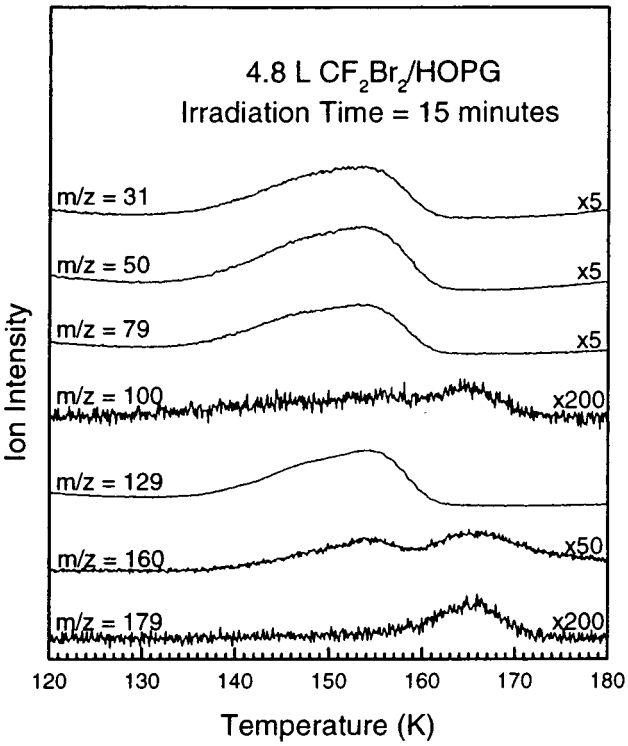

Figure 4. Temperature-programmed desorption data for 4.8 langmuir CF_2Br_2(ad)/HOPG, after 15 min of UV irradiation. Conditions same as Figure 3.

$m/z = 160$ TPD spectrum was only observed for UV irradiation times greater than 5 min.

B. X-ray Photoelectron Spectroscopy. Figure 5 shows the F 1s and Br 3d regions for increasing UV exposure. For the unirradiated sample, the F 1s binding energy was observed at 688.4 eV similar to that of CF_2Br_2 adsorbed on sapphire.[22] As

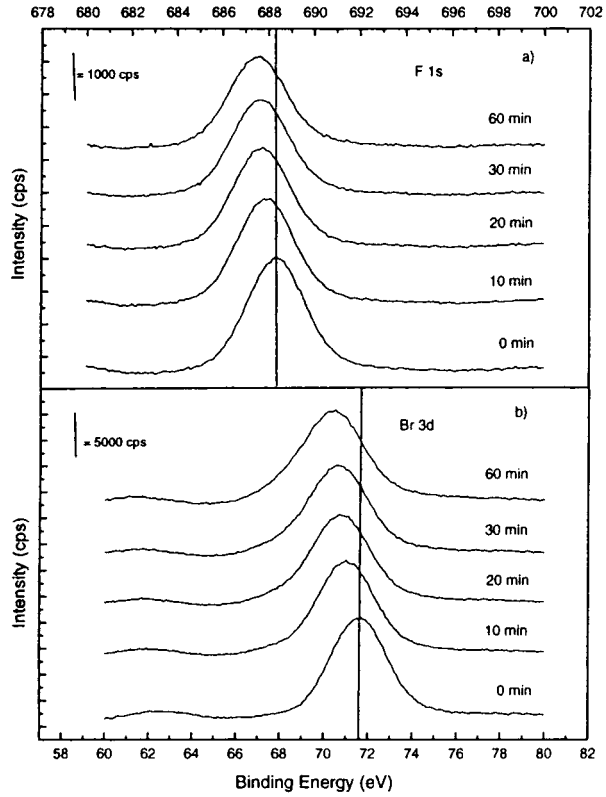

Figure 5. X-ray photoelectron spectra of F 1s region (a) and Br 3d (b) region of CF_2Br_2 monolayer as a function of UV irradiation. Vertical lines are drawn at 688.4 and 71.6 eV BE.

the UV irradiation time increased, the F 1s peak decreased in intensity and shifted to lower binding energy (687.5 eV after 60 min UV exposure) but the peak width (fwhm) remained constant at 3.0 eV. The Br 3d peak maximum (unresolved spin−orbit split doublet) was observed at 71.6 eV for the unirradiated surface. This value is relatively high compared to simple metal bromide solids (68.3−69.3 eV)[23] and about 1 eV higher than CH_3Br(ad) on Ag(111).[24] The Br 3d peak shifted to 70.4 eV and the peak broadened from 3.9 to 4.8 eV (fwhm) after 60 min of irradiation. The intensity of the Br 3d peak remained constant.

Figure 6a shows the C 1s region of the clean HOPG surface and that of a 4.8 langmuir CF_2Br_2-covered HOPG surface. The main photoemission peak in both cases is located at 284.7 eV. Furthermore, the clean graphite surface also shows the well-known shake-up feature ($\pi \rightarrow \pi^*$) centered at about 292 eV. The addition of the CF_2Br_2 monolayer resulted in an additional feature at 292.8 eV. This feature was most clearly observed in the normalized difference spectrum (bare HOPG minus 4.8 langmuir CF_2Br_2(ad)/HOPG), and was shifted by +8.1 eV BE relative to the main photoemission peak. We assign this feature to photoemission from the adsorbate carbon atom bonded to four electronegative atoms (2 F atoms and 2 Br atoms), with the majority of the observed chemical shift expected to originate from the F atoms (according to literature, approximately 2.9 eV per F atom, 1.0 eV per Br atom).[25]

Figure 6b shows XPS data of the C 1s region of a 4.8 langmuir CF_2Br_2 exposed graphite surface and an identical surface after 30 min of UV irradiation. Each spectrum represents a separate dose. After irradiation, the 292.8 eV feature was observed to decrease in intensity and a new feature appeared at approximately 290.0 eV. This is illustrated in the normalized difference spectrum shown in Figure 6b.

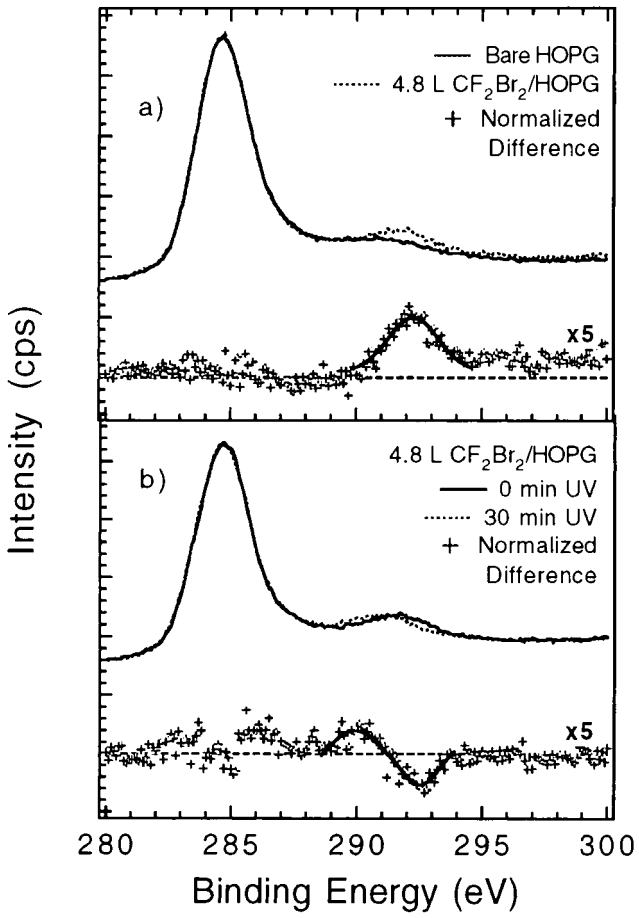

Figure 6. (a) X-ray photoelectron spectra of the C 1s region of bare HOPG (solid line), 4.8 langmuir CF_2Br_2-covered HOPG (solid circles) and the normalized difference spectrum (crosses). (b) X-ray photoelectron spectra of the C 1s region of 4.8 langmuir CF_2Br_2-covered HOPG (solid line), 4.8 langmuir CF_2Br_2-covered HOPG after 30 min UV irradiation (solid circles) and the normalized difference spectrum (crosses).

Figure 7 shows the integrated raw area ratios F 1s/C 1s and Br 3d/C 1s as a function of UV exposure. Each data point corresponds to a separate 4.8 langmuir CF_2Br_2 dose (saturated first layer). The F 1s/C 1s ratio decreased by 25% between 0 and 60 min irradiation time, suggesting a net loss of F atoms from the adlayer. In contrast, the Br 3d/C 1s ratio remained unchanged indicating that no Br atoms were expelled from the surface during UV exposure. Error bars represent 1 σ for two separate experiments.

C. Electron Energy Loss Spectroscopy. Figure 8 shows electron energy loss spectra of 4.8 langmuir of CF_2Br_2 on the HOPG surface for two different UV exposures. A spectrum of the bare HOPG surface is also shown for comparison. The spectrum for bare graphite (a) exhibited the characteristic background of a semimetal caused by excitation of low-energy electron−hole pair transitions across the Fermi level.[26] No other loss features were present in this spectrum. Spectrum (b) shows the surface exposed to 4.8 langmuir of CF_2Br_2 without UV irradiation. A weak loss was observed at 1157 cm^{-1}. We assign this feature as the CF_2 asymmetric stretch in the adsorbed molecule since it is close to the reported value for CF_2Br_2(g/s) of 1153 cm^{-1}.[27,28] Spectrum (c) shows the 4.8 langmuir CF_2Br_2/HOPG surface after 30 min of UV irradiation. Again, the only loss peak present was a C−F-like stretch that had red-shifted to 1129 cm^{-1} and gained intensity. Furthermore, a

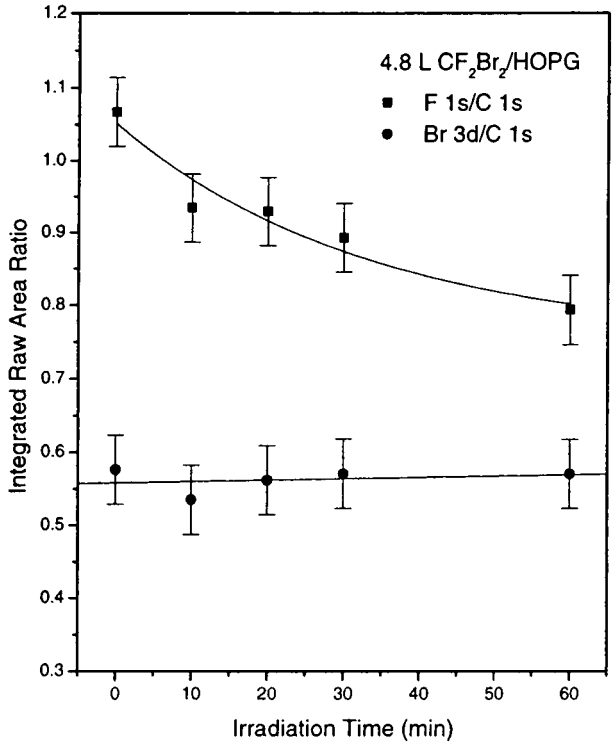

Figure 7. Integrated area ratios (F 1s/C 1s and Br 3d/C 1s) from X-ray photoelectron spectroscopy of 4.8 langmuir CF_2Br_2 adsorbed on HOPG, as a function of UV irradiation time (conditions as Figure 3). The solid curve in the F 1s/C 1s ratio is a single-exponential fit to the data. The solid curve in the Br 3d/C 1s data is a linear fit to the data.

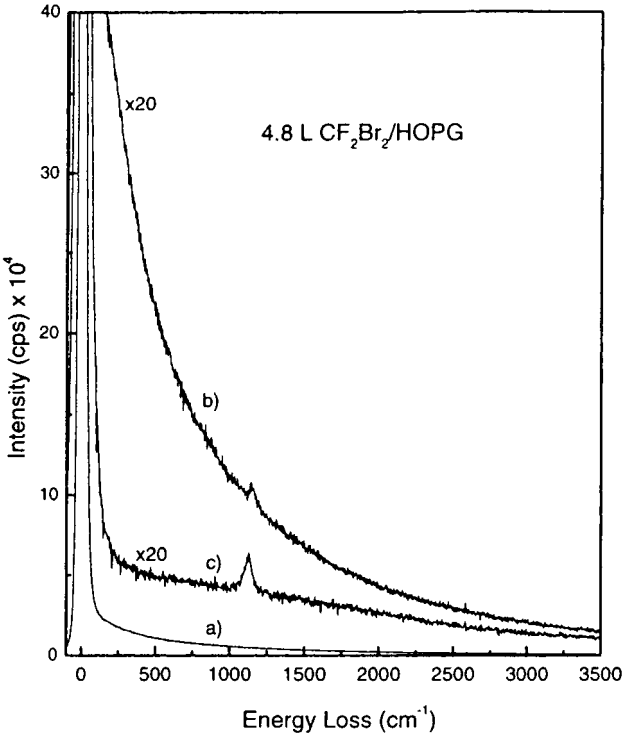

Figure 8. High-resolution electron energy loss spectra of (a) clean HOPG (b) 4.8 langmuir CF_2Br_2-covered HOPG and (c) 4.8 langmuir CF_2Br_2-covered HOPG after 30 min UV irradiation.

noticeable decrease in the overall background intensity was observed.

IV. Discussion

A. Adsorption and Desorption of CF_2Br_2(ad)/HOPG. The TPD data in Figures 1 and 2 show that CF_2Br_2 undergoes molecular adsorption and desorption from a clean HOPG surface in the absence of UV irradiation. The measured ion abundances for m/z = 31, 50, 79, and 129 in our desorption data closely match those of CF_2Br_2(g). For the adsorbed layer, apparent zero-order desorption kinetics were observed. Such behavior can arise either through true zero-order desorption kinetics, first-order desorption kinetics modified by attractive interadsorbate interactions or half-order desorption kinetics from 2-D islands modified by attractive interadsorbate interactions.[29−31]

Knorr and co-workers[32−36] have proposed monolayer structural models based on X-ray diffraction data for many halocarbons (but not CF_2Br_2) on graphite. Their data for CF_2Cl_2 indicated coexistence of a two-dimensional island (β phase) and lattice gas phase at the temperatures and coverages appropriate to our measurements. It was suggested that the presence of the permanent dipole moment in CF_2Cl_2 favored either an antiparallel or zigzag arrangement of dipoles within the islands. We believe that the zero-order desorption kinetics observed in our TPD experiments for the first layer of CF_2Br_2 are also consistent with the formation of 2-D islands modified by attractive interadsorbate interactions.[29−31] Similar TPD behavior has also been observed for H_2O adsorption on HOPG surfaces, and attributed to the creation of 2-D islands nucleated at defect sites.[37] We speculate that the lower temperature desorption feature (~110 K), characteristic of multilayer desorption, appears after the 2-D islands in the monolayer coalesce.

To our knowledge, the structure of the CF_2Br_2 monolayer on graphite has not been determined. However, some information on a possible structure can be obtained by comparing the fractional coverage, ΦCF_2Br_2 (defined as the number of adsorbate molecules per surface C atom), with the fractional coverage of CF_2Cl_2 on graphite. In our case, the fractional coverage was calculated for CF_2Br_2 on HOPG using the XPS integrated raw area ratios shown in Figure 7 and expressions developed in the literature.[25] Using sensitivity factors appropriate for our electron analyzer (C 1s = 0.205, F 1s = 1.00 and Br 3d = 0.59[23]), a mean value of $\Phi CF_2Br_2 = 0.14 \pm 0.01$ (4.6×10^{14} molecules/cm^2) was obtained.

The calculated fractional coverage compares favorably to the maximum fractional coverage of the β phase of CF_2Cl_2 on graphite ($\Phi CF_2Cl_2 = 0.137$).[33,36] Similar surface structures for monolayers of CF_2Cl_2 and CF_2Br_2 may be anticipated based on the similarity of their dipole moments (CF_2Cl_2 = 0.51 D, CF_2Br_2 = 0.66 D)[38] and projected surface areas (CF_2Cl_2 = 27.9 Å^2, CF_2Br_2 = 31.7 Å^2). Areas were estimated from van der Waals' radii assuming both molecules have one F and two X atoms (X = Cl, Br) in contact with the surface (CFX_2 "tripod").[32−36] The EELS data shown in Figure 8b provides additional evidence for this adsorption geometry. The appearance of a single vibrational mode at 1157 cm^{-1}, corresponding to the CF_2 asymmetric stretch (1153 cm^{-1}, b_1 symmetry in CF_2Br_2(g)), is consistent with a CF_2 plane that is not parallel to the HOPG surface (surface selection rule). The companion $\nu_s(CF_2)$ mode of CF_2Br_2 expected at ~1090 cm^{-1} was not observed, presumably due to a small component of the dynamic dipole parallel to the surface normal. No loss features attributable to CBr_2 vibrations were observed.

B. Photolysis of CF_2Br_2 on HOPG. Numerous studies have shown the initial photodissociation step operative at 200−300 nm in CF_2Br_2(g), is C−Br bond cleavage in a single photon process.[39−50]

$$CF_2Br_2 + h\nu \rightarrow CF_2Br + Br \quad (1)$$

Similarly, upon exposure to UV radiation, photolysis of the CF_2-

Br_2 adsorbed on graphite was observed. The $m/z = 129$ TPD data of Figures 3 and 4 showed a decreased intensity of the 138−141 K peak associated with molecularly adsorbed CF_2Br_2 for increasing UV irradiation times. The dissociation cross section for CF_2Br_2(ad)/graphite was estimated by measuring this loss in intensity as a function of UV exposure. For the range of wavelengths generated by our filtered arc lamp, the apparent total cross section (the integrated cross section for 225−350 nm) was 1.9×10^{-19} cm^2 (using a mean wavelength of 287.5 nm in the calculation). Similarly, we estimated the integrated cross section for CF_2Br_2(g) over the same range of wavelengths by multiplying the scaled irradiance curve for our lamp,[51] the $NiSO_4$ filter transmission spectrum[52] and the gas-phase cross section data.[53,54] The integrated cross section (225−350 nm) for CF_2Br_2(g) was 4.5×10^{-19} cm^2, very similar to our CF_2Br_2(ad)/HOPG value. In fact, greater than 95% of the contribution to the cross section occurs in the 240−250 nm region (where the Hg lamp irradiance is high and the cross section for CF_2Br_2(g) is large). Absorption cross sections for wavelengths greater than 250 nm decrease rapidly ($\sim 10^{-19}$ cm^2 at 250 nm to $\sim 10^{-23}$ cm^2 at 320 nm).[53,54] Essentially, no contribution to the photolysis of CF_2Br_2 is expected for wavelengths greater than 320 nm. There was no evidence for photochemical modification of CF_2Br_2 monolayers by ambient (visible) light entering the UHV chamber.

The EELS data shown in Figure 8c indicated that after UV irradiation the loss originally present at 1157 cm^{-1}, due to CF_2 ν_{as} in CF_2Br_2(ad), became more intense and red-shifted to 1129 cm^{-1}. This value is very close to that observed in a study of the 254 nm photolysis of CF_2Br_2 in an Ar matrix (1138 cm^{-1}).[39] In that study, a definitive symmetry could not be assigned to this mode but it was assigned to one of the fundamental C−F stretches of CF_2Br. The similarity of the integrated cross-sectional data for CF_2Br_2(ad)/HOPG and CF_2Br_2(g), and the observation of a vibrational mode of CF_2Br(ad), implies that UV irradiation of dibromodifluoromethane produces surface-bound CF_2Br in a fashion similar to eq 1.

Further evidence for photochemistry of the adsorbed CF_2Br_2 is observed by a shift in the C 1s photoemission peak (Figure 6), from 292.8 to 290.0 eV BE following UV exposure. The direction of the shift suggests a net reduction in the number of electronegative substituent atoms attached to the C atom of CF_2Br_2(ad). The magnitude of the shift (−2.8 eV) is consistent with loss of an F atom to produce $CFBr_2$(ad), but we believe that this to be misleading. The shift must correspond to loss of a single Br atom to form CF_2Br(ad), as clearly observed in EELS and TPD measurements. The large C 1s BE shift observed following photolysis is likely to be complicated by changes in the intensity of the C 1s shake-up feature at ~292 eV. This feature is sensitive to the electronic structure of the surface. Indeed, based on analogy with bromine-intercalated graphite compounds, the presence of Br on the graphite surface is expected to cause some charge transfer from the graphite to the Br atoms.[55] This would cause a decrease in the population of the filled graphite π-band and an increase in electronic conductivity.[56] The decrease in the electron−hole pair background in our EELS data (Figure 8) also supports the idea of a more metallic surface for UV-irradiated CF_2Br_2 on graphite.

It is somewhat surprising that electron-induced chemistry due to photon absorption by graphite does not appear to significantly contribute to the observed photochemistry of CF_2Br_2(ad). Graphite strongly absorbs in the UV generating free photoelectrons with kinetic energies from 0 to about 0.7 eV ($h\nu_{250\ nm} = 5.0$ eV, graphite work-function, $\Phi = 4.35$ eV[57]). These do not appear to cause dissociative electron attachment-type reactions for the adsorbed molecule despite the fact that for gas-phase CF_2Br_2, a large dissociative electron attachment cross section of $>10^{-15}$ cm^2 is observed for ~0 eV electrons.[58] There is substantial evidence in the literature that, in general, low energy electrons generated by photon irradiation of metallic and semiconductor surfaces can cause dissociation of an adsorbed molecule.[16] The apparent lack of electron-induced chemistry for adsorbed CF_2Br_2 is likely due to either an increased work-function for graphite upon adsorption (>0.7 eV), poor spatial/energetic overlap between the graphite and adsorbate orbitals or competitive quenching by the surface.

C. Surface Recombination Reactions. In static cell studies of the photolysis of CF_2Br_2(g) a variety of radicals and stable molecules are generated, including CF_2Br, CF_2, Br and $C_2F_4Br_2$ (formed by biradical reaction of CF_2Br).[41−43,45,47−50] Reactions generating Br_2 and C_2F_4 do not appear to be major product channels at wavelengths greater than about 248 nm and at low photon fluences.

The high temperature (155 K) TPD feature observed in our data is likely due to recombination of photogenerated CF_2Br(ad) and Br(ad) atoms during the TPD experiment. The photodissociation event imparts kinetic energy to the nascent photofragments (total up to about 2.0 eV at our shortest wavelength), separating them and preventing immediate recombination. Prompt recombination would generate CF_2Br_2 that would be indistinguishable in TPD measurements from the unphotolyzed molecules. We assume CF_2Br and Br are weakly chemisorbed and not significantly mobile, since they are stable on the graphite surface up to ~155 K. Diffusion of one or both of these species apparently occurs only at the elevated surface temperatures experienced during TPD.

Another recombination product observed on the HOPG surface was Br_2(ad) as indicated by the appearance of a desorption peak centered at 165 K for $m/z = 160$ (Figure 4). This feature is observed only after extended UV irradiation periods (≥10 min). The expected $m/z = 79$ ion (Br^+) at 165 K from fragmentation of Br_2 in the ionizer has a small abundance, preventing detection in our data (see Figure 4). It should be noted that the appearance of coincident features in the $m/z = 100$ and 179 are not related to the production of Br_2(ad) but are associated with another photolysis product, $C_2F_4Br_2$ (see below).

Molecular bromine can result from concerted or sequential elimination from a single CF_2Br_2 molecule

$$CF_2Br_2 + h\nu \rightarrow CF_2 + Br_2 \qquad (2)$$

or

$$CF_2Br_2 + h\nu \rightarrow CF_2Br + Br$$
$$CF_2Br + h\nu \rightarrow CF_2 + Br$$
$$Br + Br \rightarrow Br_2 \qquad (3)$$

or from the recombination of Br atoms produced from photolysis of two CF_2Br_2 molecules

$$2CF_2Br_2 + 2h\nu \rightarrow 2CF_2Br + 2Br$$
$$Br + Br \rightarrow Br_2 \qquad (4)$$

Even at the shortest wavelengths employed here, there is insufficient energy in a single photon ($h\nu_{250\ nm} = 5.0$ eV) to simultaneously cleave two C−Br bonds ($2 \times D_0(C-Br) \cong 6.0$ eV).[38] Therefore, we discount reaction 2 as the source of Br_2.

The photodissociation cross section of $CF_2Br(g)$ is $(0.5-4.4) \times 10^{-18}$ cm^2 at 248 nm,[45,47-49] about an order of magnitude greater than the value for $CF_2Br_2(g)$ at the same wavelength. As such we anticipate significant photodissociation of the CF_2Br photoproduct to occur. We found no evidence for the formation of CF_2(ad), however, the formation of CF_2(g) which is expelled from the adlayer following photolysis of CF_2Br(ad), does not preclude the formation of adsorbed Br. We are therefore unable to comment on the relative contributions of reactions 3 and 4 to the production of Br atoms.

The XPS data indicated Br-containing species formed during UV irradiation of CF_2Br_2 remained adsorbed on the surface, as shown in Figure 7. Consistent with the production of several species (CF_2Br, Br, Br_2, $C_2F_4Br_2$) during photolysis, the Br 3d peak broadened from 3.9 to 4.8 eV fwhm between 0 and 60 min irradiation, respectively. The peak center also shifted from 71.6 to 70.4 eV BE. The shift implies a net reduction in the number of Br atoms in an electronegative environment as expected for Br and Br_2 compared with CF_2Br_2 (we assume the binding energies for Br in CF_2Br_2 and $C_2F_4Br_2$ are similar).

A second photoproduct formed was $C_2F_4Br_2$ (Halon 2402) by dimerization of two photogenerated CF_2Br radicals. The dimer is indicated by the appearance of desorption peaks at ~165 K for $m/z = 100$ ($C_2F_4^+$) and 179 ($C_2F_4Br^+$), as shown in Figures 3 and 4. The measured TPD intensity ratio at these two masses (47:100 for $m/z = 100$ and 179, respectively) agrees with our measured QMS ion abundances for $C_2F_4Br_2(g)$ (43:100 for $m/z = 100$ and 179, respectively), confirming the presence of $C_2F_4Br_2$(ad).

It should be noted that the unirradiated CF_2Br_2 monolayer showed a small TPD peak at ~141 K for $m/z = 100$. This is believed to be an impurity; there is no peak at this m/z in the mass spectrum of $CF_2Br_2(g)$.[59] It is unlikely that any Br (or Br_2) is contributed by the direct photolysis of $C_2F_4Br_2$. Ultraviolet photodissociation cross sections for $C_2F_4Br_2(g)$ at the wavelengths used in our experiments (225−350 nm) are quite small (~$10^{-20}-10^{-21}$ cm^2).[53,54]

D. Loss of Fluorine Species. The total loss of parent CF_2Br_2 as determined from TPD measurements (~140 K peak), was approximately 14 ± 3% after 15 min irradiation. This value is almost identical to the decrease in the F 1s/C 1s XPS intensity ratio after the same UV irradiation period (13 ± 5%). However, it will be recalled that there was essentially no change in the Br 3d/C 1s XPS intensity ratio over this (or extended) UV exposures. This immediately implies that the observed loss of fluorine-containing species cannot be due to photodesorption of CF_2Br_2 or CF_2Br, both of which would reduce the total Br concentration on the surface.

In addition to CF_2Br, both CF_2 and C_2F_4 products have been observed in matrix isolation experiments of CF_2Br_2 photochemistry.[39] Although we see no evidence for CF_2(ad) in our EELS data, it is possible that the CF_2 formed during photolysis of CF_2Br is expelled from the surface as CF_2(g). The formation of CF_2(ad) would be signaled by the appearance of vibrational modes at ~1225 cm^{-1} ($\nu_s - a_1$ symmetry) and ~1106 cm^{-1} ($\nu_{as} - b_1$ symmetry).[59] Alternatively, CF_2 photofragments may combine to produce C_2F_4(ad) or C_2F_4(g). We can discount the formation of appreciable quantities of C_2F_4(ad) since at no time did we observe features in the EELS data due to C_2F_4(ad) (~1180 and 1330 cm^{-1})[59] or in TPD data attributable to the cracking of C_2F_4 (notably at $m/z = 31$ and 100).[59]

In principle, it should be possible to determine the overall stoichiometry of the departing fluorine-containing species by examining the reduction in the ~293 eV feature in the C 1s XP spectrum (Figure 6) with UV exposure. However, the difficulties associated with background subtraction and the relative weakness of the feature (the number of C atoms possibly leaving the surface as CF_2(g) is very small compared to the number of C atoms sampled in the HOPG) made the results unreliable. A shift in binding energy (−0.9 eV after 60 min UV irradiation) was observed for the F 1s peak, presumably due to net loss of the Br atom. In contrast to the Br 3d peak, the F 1s peak exhibited no discernible broadening, implying that only one type of F chemical environment was present on the surface after extended photolysis. The remaining species, CF_2Br and $C_2F_4Br_2$, both contain similar bonding arrangements for F so different binding energies for these adsorbates are not expected.

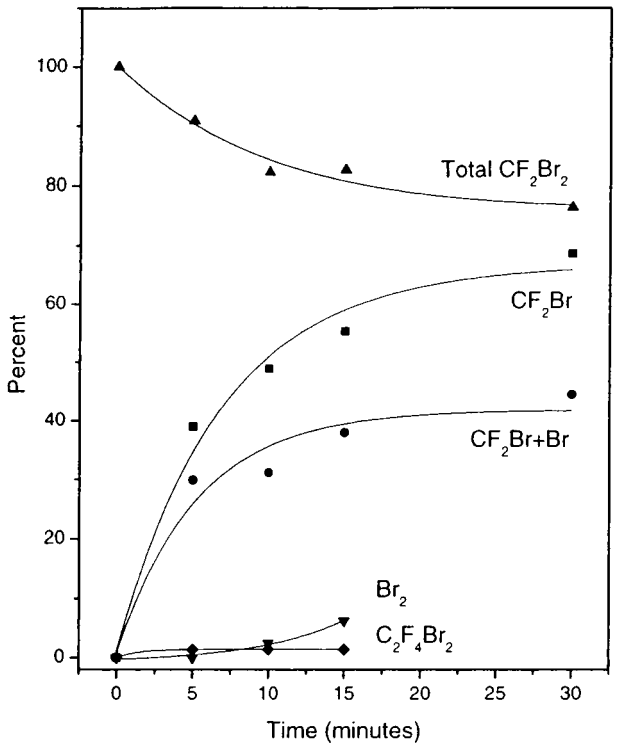

Figure 9. Relative percentages of the different reaction channels present on the surface as a function of UV irradiation. The lines through the data are guides to the eye.

Several authors have studied the photodissociation of $CF_2Br_2(g)$ and determined that approximately 20−30% of the CF_2Br formed following the initial CF_2Br_2 photolysis undergoes a second C−Br scission via a vibrationally excited CF_2Br^* radical.[45,46,48] This process generates a second Br atom and a CF_2 radical. Such a scenario is also consistent with our observations for loss of fluorine from CF_2Br_2(ad)/graphite (see Figure 7) if the vibrationally excited CF_2Br^* subsequently fragments to produce CF_2(g) and Br(ad). Indeed, the rate of loss of F-containing species is, on average, 25% the rate of dissociation of CF_2Br_2(ad)/graphite (Figure 9), which is in good agreement with the value of Gosnell et al.[45] Experimental geometry prevented us from directly monitoring species desorbing during irradiation and we cannot independently confirm desorption of CF_2(g) from the adlayer in our case.

E. Quantification of Surface Reactions. Calculations were performed based on our TPD data in order to quantify the various products on the HOPG surface after UV irradiation. Electron impact ionization cross sections were calculated for CF_2Br_2, Br_2, and $C_2F_4Br_2$ using Deutsch-Märk (D−M) theory[60] in order to correct for ionization efficiency of the products at

the electron energy of our QMS (70 eV). Deutsch-Märk theory is a semiclassical approach based on quantum-mechanically calculated molecular structure, population weighting factors and summed contributions arising from electron ejection by each occupied molecular orbital. Of the various calculation schemes used to determine absolute electron impact ionization cross sections, D−M theory appears to give the most reliable results for molecules containing heavy atoms.[61] The calculated electron impact ionization cross sections were $CF_2Br_2 = 11.25$ Å^2, $Br_2 = 7.78$ Å^2 and $C_2F_4Br_2 = 14.48$ Å^2.[62] Corrections were also made for ion fragmentation using published and measured mass spectra for CF_2Br_2(g), Br_2(g) and $C_2F_4Br_2$(g).[59]

Figure 9 summarizes the relative rates of the various processes observed during UV irradiation of 4.8 langmuir CF_2Br_2(ad)/HOPG, after correction for electron impact ionization cross sections and fragmentation. The most prominent reaction channel for all UV exposures studied was the C−Br photodissociation event as shown in eq 1. For example, after 15 min of UV irradiation, the monolayer is composed of approximately 45 ± 7% unphotolyzed and 55 ± 7% photolyzed CF_2Br_2 molecules. During temperature-programmed desorption experiments, most of the photolyzed molecules (70 ± 10% of the photolyzed fraction or 38 ± 6% of the total CF_2Br_2 molecules) recombine to regenerate parent molecules (155 K peak in TPD data). The remainder of the photolyzed molecules (30 ± 5% of the photolyzed fraction or 17 ± 3% of the total CF_2Br_2 molecules) form other reaction products. The fluorine-containing component of this remaining 17 ± 3% appears to be almost completely lost from the adlayer (as indicated by both F 1s/C 1s XPS and $m/z = 129$ TPD data). The formation of $C_2F_4Br_2$ and Br_2 increased to 1.4 ± 0.6% and 6 ± 2% of the total number of molecules, respectively, after 15 min of irradiation, indicating that recombination of CF_2Br radicals and Br atoms are relatively minor channels.

We observe various recombination reactions during TPD measurements due to the formation of an adlayer with a high density of photogenerated radicals. However, we observe reaction probabilities that are significantly different to those observed for the photolysis of CF_2Br_2(g). The most prevalent reaction observed in our experiments was the recombination of a large fraction of the photolyzed molecules to reform the parent during heating in TPD measurements, a channel not detected in static-cell gas phase[41−43,45,47−50] or (low temperature) matrix isolation[39] studies. Vatsa et al.[49] have suggested that the majority (90%) of the CF_2Br radicals produced by 248 nm photodissociation of CF_2Br_2(g) in a cell formed $C_2F_4Br_2$ through dimerization reactions. We observed that the formation of $C_2F_4Br_2$ was a minor channel on the surface reaching a maximum after 10 min of photolysis. The proportions of the various products are not simply statistical if only CF_2Br and Br are produced. In this case, we would expect the formation of equimolar amounts of Br_2 and $C_2F_4Br_2$. The formation of a higher amount of Br_2 than expected (by about a factor of 4 compared to $C_2F_4Br_2$) is likely due to efficient photolysis of CF_2Br(ad), spontaneous C−Br scission in CF_2Br* or other controlling factors operative on the surface. Surface processes may include reduced reaction probability for a particular recombination, perhaps due to structural (orientational) constraints, or reduced surface diffusion for one of the species.

V. Conclusions

Dibromodifluoromethane (CF_2Br_2) adsorbed molecularly on an HOPG surface at 85 K, with monolayer saturation corresponding to a fractional coverage of 0.14 ± 0.01 CF_2Br_2 per surface C atom. Molecular desorption occurred from the monolayer at approximately 138−141 K. Photolysis of CF_2Br_2 was observed upon exposure to 225−350 nm Hg arc lamp irradiation. The major products formed during photolysis were CF_2Br and Br atoms. The estimated integral cross section (225−350 nm) for this process was $\sim 1.9 \times 10^{-19}$ cm^2, similar to the integrated UV photolysis cross section for CF_2Br_2(g) at these wavelengths. This implies that dissociative electron attachment (DEA) does not significantly contribute to the adsorbate photochemistry. A large fraction of the CF_2Br and Br recombine to produce CF_2Br_2 during TPD experiments. Additionally, minor channels for Br_2 and $C_2F_4Br_2$ (Halon 2402) formation were observed. It should be noted that the adsorption/desorption temperatures observed for all species in our work are 30−50 K lower than the minimum temperatures of the upper troposphere or lower stratosphere. Within the validity of our HOPG surface as an accurate model for primary carbon aerosols, the observed reactions will be negligible in the atmosphere.

Acknowledgment. The authors would like to thank Dr. Klaus Knorr for helpful discussions regarding coverages and structures for halogenated methanes on graphite and Dr. Peter W. Harland for graciously providing the calculated DM electron impact ionization cross sections. M.J.D. would like to thank the Michigan Space Grant Consortium (NASA) for award of a fellowship.

References and Notes

(1) Quinlan, M. A.; Reihs, C. M.; Golden, D. M.; Tolbert, M. A. *J. Phys. Chem.* **1990**, *94*, 3255.
(2) Tolbert, M. A.; Rossi, M. J.; Malhotra, R.; Golden, D. M. *Science* **1987**, *238*, 1258.
(3) Donsig; H. A.; Herridge, D.; Vickerman, J. C. *J. Phys. Chem. A* **1999**, *103*, 9211.
(4) Berland, B. S.; Tolbert, M. A.; George, S. M. *J. Phys. Chem. A* **1997**, *101*, 9954.
(5) Finlayson-Pitts, B. J.; Pitts, J. N., Jr. *Chemistry of the Upper and Lower Atmosphere;* Academic Press: San Diego, 2000; p 701.
(6) Schauffler, S. M.; Atlas, E. L.; Flocke, F.; Lueb, R. A.; Stroud, V.; Travnicek, W. *Geophys. Res. Lett.* **1998**, *25*, 317.
(7) Molina, M. J.; Molina, L. T.; Kolb, C. E. *Annu. Rev. Phys. Chem.* **1996**, *47*, 327.
(8) United Nations Environmental Program. *Montreal Protocol on Substances That Deplete the Ozone Layer*; Montreal, 1987.
(9) Fraser, P. J.; Oram, D. E.; Reeves, C. E.; Penkett, S. A.; McCulloch, A. M. *J. Geophys. Res.* **1999**, *104*, 15985.
(10) Zhang, R.; Jayne, J. T.; Molina, M. J. *J. Phys. Chem.* **1994**, *98*, 867.
(11) Roberts, J. T. *Acc. Chem. Res.* **1998**, *31*, 415.
(12) Oum, K. W.; Lakin, M. J.; DeHaan, D. O.; Brauers, T.; Finlayson-Pitts, B. J. *Science* **1998**, *279*, 74.
(13) Hemminger, J. C. *Int. Rev. Phys. Chem.* **1999**, *18*, 387.
(14) DeHaan, D. O.; Brauers, T.; Oum, K.; Stutz, J.; Nordmeyer, T.; Finlayson-Pitts, B. J. *Int. Rev. Phys. Chem.* **1999**, *18*, 343.
(15) Andreae, M. O.; Crutzen, P. J. *Science* **1997**, *276*, 1052.
(16) Zhou, X.-L.; Zhu, X.-Y.; White, J. M. *Surf. Sci. Rep.* **1991**, *13*, 73.
(17) Bryden, T. R.; Garrett, S. J. *J. Phys. Chem. B* **1999**, *103*, 10481.
(18) Musket, R. G.; McLean, W.; Colmenares, C. A.; Makowiecki, D. M.; Siekhaus, W. J. *Appl. Surf. Sci.* **1982**, *10*, 143.
(19) Barr, T. L. *Modern ESCA: The Principles and Practice of X-ray Photoelectron Spectroscopy*; CRC Press: Boca Raton, FL, 1994; p 209.
(20) de Jong, A. M.; Niemantsverdriet, J. W. *Surf. Sci.* **1990**, *233*, 355.
(21) Yates, J. T., Jr. *Methods of Experimental Physics*; Academic Press: San Diego, 1985; Vol. 22, p 425.
(22) Robinson, G. N.; Freedman, A.; Kolb, C. E.; Worsnop, D. R. *Geophys. Res. Lett.* **1994**, *21*, 377.
(23) Wagner, C. D., Riggs, W. M., Davis, L. E., Moulder, J. F., Mullenburg, G. E., Eds. *Handbook of X-ray photoelectron Spectroscopy*; Perkin-Elmer Corp.: Eden Prairie, MN, 1979; p 94.
(24) Zhou, X.-L.; White, J. M. *Surf. Sci.* **1991**, *241*, 259.
(25) Briggs, D. In *Practical Surface Analysis*; Briggs, D.; Seah, M., Eds.; Wiley and Sons: New York, 1990; Vol. 1, p 444.
(26) Palmer, R. E.; Annett, J. F.; Willis, R. F. *Phys. Rev. Lett.* **1987**, *58*, 2490.
(27) Eix, S. L.; Schlueter, S. A.; Anderson, A. *J. Raman Spectrosc.* **1992**, *23*, 495.

(28) Baldacci, A.; Gambi, A.; Giorgianni, S.; Visinoni, R.; Ghersetti, S. *Spectrochim. Acta* **1987**, *43A*, 455.
(29) Golze, M.; Grunze, M.; Hirschwald, W *Vacuum* **1981**, *31*, 697.
(30) Niemantsverdriet, J. W.; Markert, K.; Wandelt, K. *Appl. Surf. Sci.* **1988**, *31*, 211.
(31) Zhou, X.-L.; White, J. M.; Koel, B. E. *Surf. Sci.* **1989**, *218*, 201.
(32) Knorr, K. *Phys. Rep.* **1992**, *214*, 113.
(33) Knorr, K.; Civera-Garcia, E. *Surf. Sci.* **1990**, *232*, 203.
(34) Nalezinski, R.; Bradshaw, A. M.; Knorr, K. *Surf. Sci.* **1995**, *333*, 255.
(35) Volkmann, U. G.; Knorr, K. *Phys. Rev.* B **1993**, *47*, 4011.
(36) Warken, A.; Enderle, M.; Knorr, K. *Phys. Rev. B* **2000**, *61*, 3028.
(37) Chakarov, D. V.; Österlund, L.; Kasemo, B. *Vacuum* **1995**, *46*, 1109.
(38) Lide, D. R., Ed.; *CRC Handbook of Chemistry and Physics*, 75th ed.; CRC Press: Boca Raton, FL, 1995.
(39) Jacox, M. E. *Chem. Phys. Lett.* **1977**, *53*, 192.
(40) Johnson, C. A. F.; Ross, H. J. *J. Chem. Soc., Faraday Trans. 1* **1978**, *74*, 2930.
(41) Sam, C. L.; Yardley, J. T. *Chem. Phys. Lett.* **1978**, *61*, 509.
(42) Wampler, F. B.; Tiee, J. J.; Rice, W. W.; Oldenborg, R. C. *J. Chem. Phys.* **1979**, *71*, 3926.
(43) Molina, L. T.; Molina, M. J. *J. Phys. Chem.* **1983**, *87*, 1306.
(44) Krajnovich, D.; Zhang, Z.; Butler, L.; Lee, Y. T. *J. Phys. Chem.* **1984**, *88*, 4561.
(45) Gosnell, T. R.; Taylor, A. J.; Lyman, J. L. *J. Chem. Phys.* **1991**, *94*, 5949.
(46) Talukdar, R. K.; Vaghijani, G. L.; Ravishankara, A. R. *J. Chem. Phys.* **1992**, *96*, 8194.
(47) Vatsa, R. K.; Kumar, A.; Naik, P. D.; Rama Rao, K. V. S.; Mittal, J. P. *Chem. Phys. Lett.* **1993**, *207*, 75.
(48) Van Hoeymissen, J.; Uten, W.; Peeters, J. *Chem. Phys. Lett.* **1994**, *226*, 159.
(49) Vatsa, R. K.; Kumar, A.; Naik, P. D.; Rama Rao, K. V. S.; Mittal, J. P. *Bull. Chem. Soc. Jpn.* **1995**, *68*, 2817.
(50) Talukdar, R. K.; Hunter, M.; Warren, R. F.; Burkholder, J. B.; Ravishankara, A. R. *Chem. Phys. Lett.* **1996**, *262*, 669.
(51) Esposito, E., Fernandes, N., FitzSimons, C., Marino, E., III, Eds. *Light Sources, Monochromators and Spectrographs, Detectors and Detection Systems, and Fiber Optics*; Oriel Corporation: Stratford, 1994; Vol. 2, pp 1−42.
(52) Calvert, J. G.; Pitts, J. N., Jr. *Photochemistry*; Wiley and Sons: New York, 1966; p 729.
(53) Orkin, V. L.; Kasimovskaya, E. E. *J. Atmos. Chem.* **1995**, *21*, 1.
(54) Burkholder, J. B.; Wilson, R. R.; Gierczak, T.; Talukdar, R.; McKeen, S. A.; Orlando, J. J.; Vaghjiani, G. L.; Ravishankara, A. R. *J. Geophys. Res.* **1991**, *96*, 5025.
(55) Ellis, A. B.; Geselbracht, M. J.; Johnson, B. J.; Lisensky, G. C.; Robinson, W. R. *Teaching General Chemistry: A Materials Science Companion*; American Chemical Society: Washington, DC, 1993; p 193.
(56) Burdett, J. K. *Chemical Bonding in Solids*; Oxford: New York, 1995; p 71.
(57) Somorjai, G. A. *Introduction to Surface Chemistry and Catalysis*; Wiley and Sons: New York, 1994; p 381.
(58) Underwood-Lemons, T.; Gergel, T. J.; Moore, J. H. *J. Chem. Phys.* **1995**, *102*, 119.
(59) N. M. S. D. Center; S. Stein, In *NIST Chemistry WebBook, NIST Standard Reference Database Number 69*; Mallard, W., Linstrom, P., Eds.; National Institutes of Standards and Technology: Gaithersburg, MD, 1998 (http://webbook.nist.gov).
(60) Deutsch, H.; Becker, K.; Märk, S.; Mærk, T. D. *Int. J. Mass Spec.* **2000**, *197*, 37.
(61) Vallance, C.; Harris, S. A.; Hudson, J. E.; Harland, P. W. *J. Phys. B* **1997**, *30*, 2465.
(62) Harland, P. W. Personal communication.